Journal of Alloys and Compounds 509 (2011) 4765–4768

Contents lists available at ScienceDirect

Journal of Alloys and Compounds

journal homepage: www.elsevier.com/locate/jallcom

Synthesis and rate performance of lithium vanadium phosphate as cathode material for Li-ion batteries

Bing Huang[a,*], Xiaoping Fan[b], Xiaodong Zheng[a], Mi Lu[a]

[a] Laboratory of Clean Energy, Department of Chemistry and Chemical Engineering, Binzhou University, Binzhou, Shandong 256603, China
[b] Military Representative Office in ChangHong Group, Mianyang, Sichuan 621000, China

ARTICLE INFO

Article history:
Received 12 December 2010
Received in revised form 14 January 2011
Accepted 20 January 2011
Available online 3 February 2011

Keywords:
Lithium-ion batteries
Electrode materials
Lithium vanadium phosphate
Rate performance
Solid state reaction

ABSTRACT

A sphere-like carbon-coated $Li_3V_2(PO_4)_3$ composite was synthesized by carbothermal reduction method with two sessions of ball milling followed by spray-drying with the dispersant of polyethylene glycol added. The structure, particle size, and surface morphology of the cathode material were investigated via X-ray diffraction, scanning electron microscopy, and high-resolution transmission electron microscopy. Results indicate that the $Li_3V_2(PO_4)_3$/C composite has a sphere-like morphology composed of a large number of carbon-coated ultrafine particles linked together with a monoclinic structure. In the voltage range of 3.0–4.3 V, it exhibits the discharge capacities of 130 mAh g^{-1} and 100 mAh g^{-1} at 0.2 C and 20 C rates, respectively. This behavior indicates that the obtained $Li_3V_2(PO_4)_3$/C material has excellent rate capability.

1. Introduction

High-power lithium ion batteries have become the most promising energy storage devices for power tools, hybrid electric vehicles (HEVs) [1,2]. Lithium metal phosphates have now been widely recognized as new generation of cathode materials that can offer the safety, power and energy to satisfy the application for high-power lithium ion batteries [3–8]. Among the phosphates, monoclinic $Li_3V_2(PO_4)_3$ is a highly promising cathode material for high-power lithium ion batteries because it has high operate voltage, good ion mobility and high reversible capacity [9–11]. However, as most of polyanion materials, the separated $[VO_6]$ octahedral in monoclinic $Li_3V_2(PO_4)_3$ reduces the electronic conductivity of the material, which results in a poor rate capability. In order to increase the electronic conductivity of $Li_3V_2(PO_4)_3$, it is a common practice to synthesis of nano-structured and conductive materials coated materials [12–16]. And some other researches improved the electronic conductivity of $Li_3V_2(PO_4)_3$ through cation or anion substitution [17–22].

In this paper, we synthesized novel spherical $Li_3V_2(PO_4)_3$/C composites through improved synthesis method, which comprises two sessions of ball milling (before and after pre-sintering of precursor) followed by spray-drying with the addition of dispersant of polyethylene glycol 400 (PEG-400). The advantages of two sessions of ball milling and dispersant of PEG-400 are reported and the rate capability of the composites is studied in detail.

2. Experimental

According to the stoichiometry, LiH_2PO_4 (99%), NH_4VO_3 (99%) were dispersed in an aqueous solution and then ball milled for 15 h. The mixtures were dried at 100 °C, and then placed into a tube furnace and heated to 350 °C for 3 h under an argon atmosphere. Then the pre-sintered mixtures and sucrose in the amount of 25 g per mole LiH_2PO_4 (about 3 wt.% carbon) was ball milled again in ethanol for 15 h. The ball-milled mixture and PEG-400 were dispersed in ethanol to obtain an emulsion, and then the emulsion product was spray dried at 120 °C. The spray dried precursor was then heated to 800 °C at a heating rate of 5 °C min^{-1} for 10 h under an argon atmosphere to yield $Li_3V_2(PO_4)_3$/C composite.

The obtained composite was subjected to X-ray diffraction (XRD) (Philips, Panalytical X' Pert) for phase analysis using CuK_α radiation. The morphology of the sample was observed by scanning electron microscope (SEM) (S-4800, Hitachi). The nature and thickness of the coated carbon was measured using the images from a high-resolution transmission electron microscope (HR-TEM) (JEM-2100, JEOL).

The $Li_3V_2(PO_4)_3$ slurry was prepared via mixing 80 wt.% active material, 10 wt.% carbon black and 10 wt.% polyvinylidene fluoride solution in *N*-methylpyrrolidone and then was coated onto an aluminum foil over an area of 1 cm^2. The cells (CR2025 coin type) were assembled in an argon-filled glove box (Etelux). The electrolyte was 1 mol L^{-1} $LiPF_6$ in ethylene carbonate/diethylene carbonate/methyl ethyl carbonate (1:1:1, v/v/v). The cells were measured using Neware galvanostatic charge–discharge unit. Cyclic voltammetry (CV) was performed with electrochemical instrument (CHI604C, Chenhua).

3. Results and discussion

Fig. 1 shows the XRD pattern of the $Li_3V_2(PO_4)_3$ powder. The diffraction peaks of the material are similar to the previous report

* Corresponding author. Tel.: +86 543 3195583; fax: +86 543 3195583.
E-mail address: huangbingbzu@sina.com (B. Huang).

0925-8388/$ – see front matter © 2011 Elsevier B.V. All rights reserved.
doi:10.1016/j.jallcom.2011.01.151

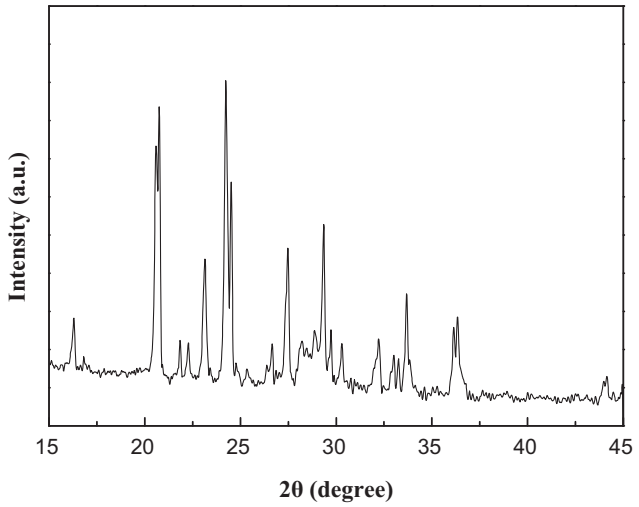

Fig. 1. XRD pattern of the $Li_3V_2(PO_4)_3$/C composite.

[7] and mainly indicate the presence of $Li_3V_2(PO_4)_3$ phase with a monoclinic structure indexed to the space group of $P2_1/n$. Excess carbon left in $Li_3V_2(PO_4)_3$/C composite was not detected most likely because there was amorphous or a low content of crystalline carbon in the samples.

SEM image of $Li_3V_2(PO_4)_3$/C sample is shown in Fig. 2, this suggests that the particles obtained in our experiments are several microns to tens of microns in diameter and morphology of the particles is sphere-like. To further investigate the prime particle size and carbon distribution in the powders, HR-TEM were taken and shown in Fig. 3. From the TEM image, it can be seen that the prime $Li_3V_2(PO_4)_3$ particle is nano-sized and wrapped with a carbon layer. The image embedded in Fig. 3 shows that the approximate thickness of the carbon coating in the samples has been calculated to be 4–5 nm. The HR-TEM images show that the modified process with two sessions of ball milling (before and after pre-sintering of precursor) created ultrafine particles. The first ball milling in an aqueous solution can reduce particle size of insoluble material and make the full mix of raw materials. In particular, the second ball milling not only makes the full mix of sucrose and pre-sintered precursor but creates ultrafine particles. The followed spray-drying step bound these ultrafine particles together via sucrose to form micron-sized sphere-like particles. The addition of PEG-400 dispersant makes the particles

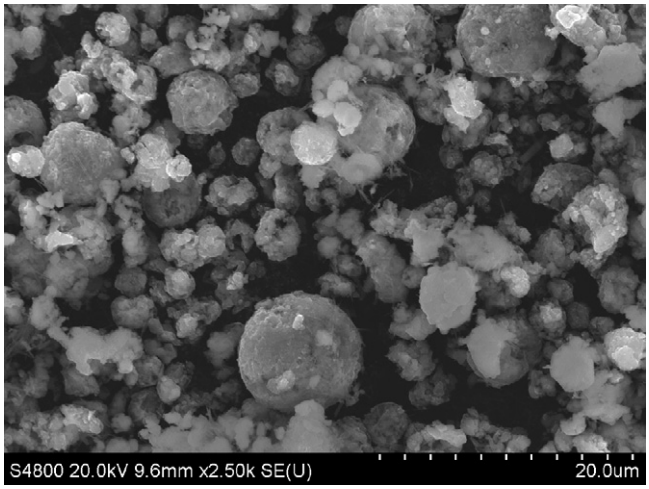

Fig. 2. SEM images of the $Li_3V_2(PO_4)_3$/C composite.

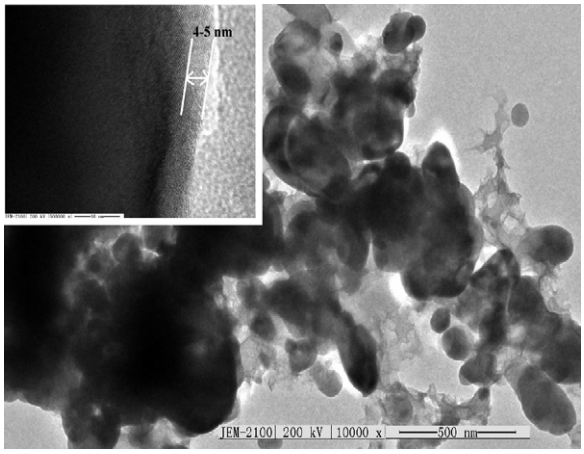

Fig. 3. TEM images of the $Li_3V_2(PO_4)_3$/C composite. Insert is a high magnification image of a $Li_3V_2(PO_4)_3$ particle and the carbon layer.

difficult to precipitate and spherical morphology of the particles after spray drying more uniform. The carbon enveloping $Li_3V_2(PO_4)_3$/C results in excellent rate performance for this material.

To find the working voltage and high-rate properties of as-prepared composite powders, the $Li_3V_2(PO_4)_3$/C electrode was discharged at different rates, which are shown in Fig. 4. The cells were charged to 4.3 V at 0.2 C rate, then discharged to 3.0 V at n C rate (where n = 0.2, 1, 5, 10, 15, 20). The initial charge–discharge profiles of the $Li_3V_2(PO_4)_3$/C electrode at 0.2 C embedded in Fig. 4 exhibit three charge plateaus and the corresponding three discharge ones, which corresponds to three compositional regions of $Li_{3-x}V_2(PO_4)_3$, that is, x = 0.0–0.5, x = 0.5–1.0 and x = 1.0–2.0. The voltage plateau in each region corresponding to the reversed two-phase transition [7] and a total discharge capacity of 130 mAh g^{-1} is achieved. As shown in Fig. 4, when the discharge current density increases from 0.2 to 5 C, the discharge capacity ratio for $Q_{5C}/Q_{0.2C}$ is 97.8%, which indicates that there is only a small capacity decrease. Even when discharging at 20 C rate, a discharge capacity of 100 mAh g^{-1} is still delivered. This should be very attractive to develop high-power lithium-ion batteries. Spherical morphology may improve the processability of the $Li_3V_2(PO_4)_3$/C cathode [8]. Carbon-coated $Li_3V_2(PO_4)_3$ ultrafine particles may increase the specific surface area of the sample and reduce the contact resis-

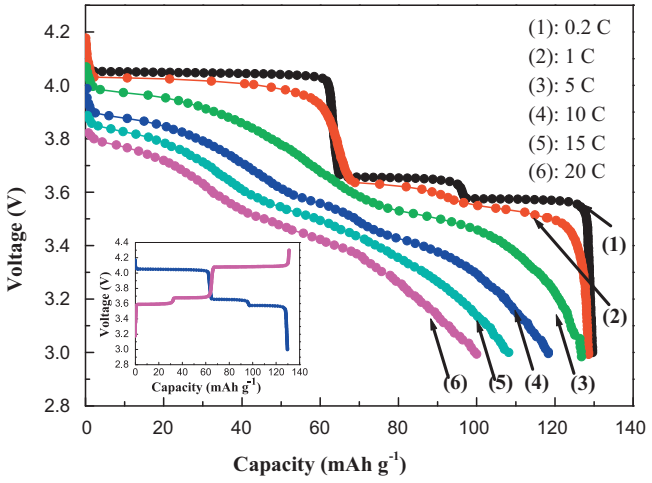

Fig. 4. Initial discharge curves of the $Li_3V_2(PO_4)_3$/C electrode at different rates. Insert is charge–discharge profiles of $Li_3V_2(PO_4)_3$/C composite material at 0.2 C rate in the voltage range of 3.0–4.3 V. (1 C = 133 mA g^{-1}).

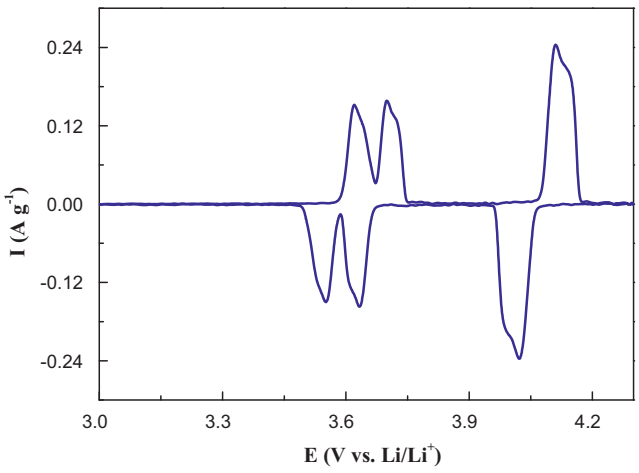

Fig. 5. Cyclic voltammetry profile of the $Li_3V_2(PO_4)_3$/C electrode.

tance of the sample, which can greatly improve the electrochemical reaction.

The charge–discharge behavior of the $Li_3V_2(PO_4)_3$ electrode may be interpreted by the CV curve in the voltage range of 3.0–4.3 V shown in Fig. 5. The CV curves of $Li_3V_2(PO_4)_3$/C composite at a scanning rate of 0.05 mV s^{-1} between 3.0 and 4.3 V (vs. Li/Li^+). As shown in Fig. 5, there are three anodic peaks at 3.62, 3.70 and 4.11 V, respectively, consistent with three charge plateaus in Fig. 4. The two peaks at 3.62 and 3.70 V correspond to the first lithium ion extraction from $Li_3V_2(PO_4)_3$ structure, and the peak at 4.11 V originates from the second lithium ion deintercalation. All the three peaks are associated with V^{3+}/V^{4+} redox couple. During the negative scan, there are correspondingly three cathodic peaks at 3.55, 3.63 and 4.02 V due to lithium insertion. Each anodic or cathodic peak in CV curve stands for two-phase transitions, which is in good agreement with the charge–discharge behavior at 0.2 C rate in Fig. 4.

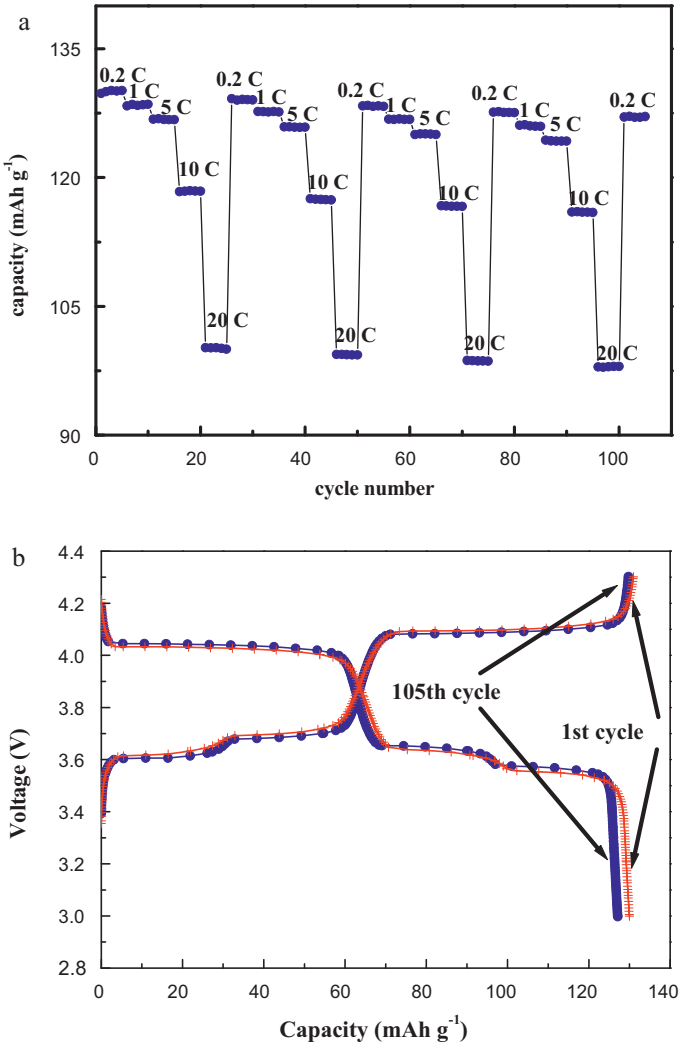

Fig. 6. (a) Cycle curves and rate performance of $Li_3V_2(PO_4)_3$/C materials and (b) charge–discharge curves of the $Li_3V_2(PO_4)_3$/C electrode at 1st and 105th cycles.

Fig. 6(a) presents the result of the cycle characterizations of the $Li/Li_3V_2(PO_4)_3$ cell at various rates from 0.2 C to 20 C and Fig. 6(b) shows the voltage–capacity profiles of the samples at 1st and 105th at 0.2 C rate. The cell exhibited excellent capacity retention as it cycled at various rates from 0.2 C to an extremely high 20 C rate. Furthermore, as shown in Fig. 6(b), the cell has similar charge–discharge plateaus in the 1st and 105th cycles and the cell delivers a high specific capacity of 127 mAh g^{-1} at 105th cycle, which is 97.7% of the 1st discharge capacity at 0.2 C rate. From the results, we conclude that the $Li_3V_2(PO_4)_3$/C composite synthesized by the improved synthesis method in this study presents excellent high-rate performance. It could be attributed to the ultrafine $Li_3V_2(PO_4)_3$ particle size and carbon coated on the surface of $Li_3V_2(PO_4)_3$ particles.

4. Conclusions

A novel sphere-like $Li_3V_2(PO_4)_3$/C composite composed of a large number of ultrafine particles linked together was synthesized via the carbothermal method with two session of ball milling followed by spray-drying. The cathode material shows a discharge capacity of 130 mAh g^{-1} at 0.2 C rate and 100 mAh g^{-1} at 20 C rate. The good rate performance makes the process promising for high performance cathode for lithium-ion batteries.

Acknowledgments

This work was supported by Doctoral Fund of Shandong Province (BS2009NJ001), the Project of Higher Educational Science and Technology Program of Shandong Province (J10LB56), and the Research Fund of Binzhou University (2008Y11 and 2008ZDL04).

References

[1] A.S. Arico, P. Bruce, B. Scrosati, J.M. Tarascon, W. Van Schalkwijk, Nat. Mater. 4 (2005) 366–377.
[2] H. Huang, T. Faulkner, J. Barker, M.Y. Saidi, J. Power Sources 189 (2009) 748–751.
[3] A.K. Padhi, K.S. Nanjundaswamy, J.B. Goodenough, J. Electrochem. Soc. 144 (1997) 1188–1194.
[4] C. Delacourt, P. Poizot, M. Morcrette, J.M. Tarascon, C. Masquelier, Chem. Mater. 16 (2004) 93–99.
[5] A. Yamada, M. Hosoya, S.C. Chung, Y. Kudo, K. Hinokuma, K.Y. Liu, Y. Nishi, J. Power Sources 119–121 (2003) 232–238.
[6] I. Belharouak, C. Johnson, K. Amine, Electrochem. Commun. 7 (2005) 983–988.
[7] M.Y. Saïdi, J. Barker, H. Huang, J.L. Swoyer, G. Adamson, J. Power Sources 119–121 (2003) 266–272.
[8] B. Huang, X. Zheng, D. Jia, M. Lu, Electrochim. Acta 55 (2010) 1227–1231.
[9] H. Huang, S.C. Yin, T. Kerr, N. Taylor, L.F. Nazar, Adv. Mater. 14 (2002) 1525–1528.
[10] L. Wang, L.C. Zhang, I. Lieberwirth, H.W. Xu, C.H. Chen, Electrochem. Commun. 12 (2010) 52–55.
[11] C.M. Burba, R. Frech, Solid State Ionics 177 (2007) 3445–3454.
[12] T. Jiang, Y.J. Wei, W.C. Pan, Z. Li, X. Ming, G. Chen, C.Z. Wang, J. Alloy Compd. 488 (2009) L26–L29.
[13] L. Zhang, X.L. Wang, J.Y. Xiang, Y. Zhou, S.J. Shi, J.P. Tu, J. Power Sources 195 (2010) 5057–5061.
[14] Y. Li, Z. Zhou, M. Ren, X. Gao, J. Yan, Electrochim. Acta 51 (2006) 6498–6502.
[15] A. Tang, X. Wang, S. Yang, Mater. Lett. 62 (2008) 3676–3678.
[16] X. Zhou, Y. Liu, Y. Guo, Electrochim. Acta 54 (2009) 2253–2258.
[17] C. Dai, Z. Chen, H. Jin, X. Hu, J. Power Sources 195 (2010) 5775–5779.

[18] J.K. Sun, F.Q. Huang, Y.M. Wang, Z.C. Shan, Z.Q. Liu, M.L. Liu, Y.J. Xia, K.Q. Li, J. Alloy Compd. 469 (2009) 327–331.
[19] S.Q. Liu, S.C. Li, K.L. Huang, B.L. Gong, G. Zhang, J. Alloy Compd. 450 (2008), 499-450.
[20] X.J. Chen, G.S. Cao, X.B. Zhao, J.P. Tu, T.J. Zhu, J. Alloy Compd. 63 (2008) 385–389.
[21] M. Ren, Z. Zhou, Y. Li, X.P. Gao, J. Yan, J. Power Sources 162 (2006) 1357–1362.
[22] Y. Chen, Y. Zhao, X. An, J. Liu, Y. Dong, L. Chen, Electrochim. Acta 54 (2009) 5844–5850.